

Supporting Information

Targeted Synthesis of core-shell Porous Aromatic Frameworks for Selective Detection of Nitro Aromatic Explosives via Fluorescence Two-Dimensional Response

Heping Ma, Bin Li, Liming Zhang, Dong Han and Guangshan Zhu*

1. Materials

2. Instruments

3. Experimental Section

4. Theoretical methods.

Figure S1: Solid-state ^{13}C NMR of PP-PAF and PP_C -PPy_S-PAF-2.

Figure S2: TGA plots of PP-PAF and PP_C -PPy_S-PAFs under air conditions.

Figure S3: XPS spectrum of PP_C -PPy_S-PAF-2.

Figure S4: Powder X-ray diffraction patterns of PP-PAF and PP_C -PPy_S-PAFs.

Figure S5: SEM images of PP-PAF and PP_C -PPy_S-PAFs.

Figure S6: a) Excitation spectra of PP-PAF, PPy-PAF and PP_C -PPy_S-PAFs, at the maximum emission, respectively; b) Absorption band of PP-PAF, PPy-PAF and PP_C -PPy_S-PAFs.

Figure S7-S11: Emission spectra of PP-PAF and PP_C -PPy_S-PAFs upon incremental addition of Cl-NB, DNT and TNT solution in ethanol.

Figure S12: Cyclic voltammograms of PP-PAF and PP_C -PPy_S-PAFs.

Figure S13: Emission spectra of PP_C -PPy_S-PAF-2 paper test strip before and after exposure to TNT vapor for 5 minutes.

Table S1. The PL and electrochemical properties of the PP-PAF, PPy-PAF and PP_C -PPy_S-PAFs

Table S2: HOMO and LUMO energies calculated for explosive analytes (at B3LYP/6-31G* level of theory).

1. Materials

All starting materials were purchased from commercial suppliers and used without further purification unless otherwise noted. benzene-1,4-diboronic acid (BDDBA), 1,3,5-Tris(4-bromophenyl)benzene (TBrPB) and tetrakis(triphenylphosphine)-palladium(0) were purchased from Sigma-Aldrich Chemicals. N, N-dimethylformamide, methanol, acetone, tetrahydrofuran and K_2CO_3 was purchased from aladdin-reagent. 1,3,6,8-tetrabromopyrene (TBrPy) were synthesized according to the reported method.^[S1]

[S1]. C. Venkataramana, S. Sankararaman, *Eur. J. Org. Chem.* 2005,19 4162-4166.

2. Instruments

FTIR spectra were obtained using an IFS 66V/S Fourier transform infrared spectrometer. Solid-state ^{13}C cross-polarization magic-angle spinning (CP/MAS) NMR were recorded on a Bruker AVANCE III 400 WB spectrometer. X-ray diffraction (XRD) measurements were carried out on a Rigaku D/MAX2550 diffractometer with Cu-K α radiation operating at a voltage of 50 kV and a current of 200

mA. The thermogravimetric analysis (TGA) was performed using a Netzsch Sta 449c thermal analyzer system at a heating rate of 10 °C/min in air atmosphere. Scanning electron microscopy (SEM) imaging was performed on JEOS JSM 6700. X-ray photoelectron spectroscopy (XPS, ESCALAB 250, Thermo Scientific) was performed by using a monochromatized Al K α (1486.6 eV) X-ray source. UV-Vis-IR diffuse reflectance spectra (Kubelka-Munk spectrum) were recorded on a HITACHI U-4100 spectrophotometer equipped with integration sphere model. Photoluminescence spectra were recorded on a HITACHI F-7000 fluorescence spectrophotometer. The absolute quantum yield was determined by standard procedure with an integral sphere mounted on the F-7000 spectrofluorometer.

The N_2 adsorption/desorption isotherms were measured on a Quantachrome Autosorb iQ2 analyzer. N_2 adsorption/desorption measurements were carried out at 77 K. Ultra-high-purity grade (99.99%) N_2 gas were used for all adsorption measurements. Liquid nitrogen bath was utilized to control the temperature at 77 K.

3. Experimental Section

Synthesis of PP-PAF: A mixture of 1,3,5-Tris(4-bromophenyl)benzene (TBrPB) (100 mg, 0.185 mmol), and benzene-1,4-diboronic acid (BDDBA) (92 mg, 0.555 mmol) in DMF (15 mL) was degassed by three freeze–pump–thaw cycles. To the mixture was added an aqueous solution of K_2CO_3 (2.0 M, 1.0 mL) and $Pd(PPh_3)_4$ (15.0 mg). The mixture was degassed by

three freeze–pump–thaw cycles, and purged with N₂, and stirred at 90 °C for 20 h. The precipitate was filtered, washed with water, methanol, THF, and DMF. Further purification was carried out by Soxhlet extraction with methanol and THF for 48 h, respectively. After dried in a vacuum oven at 150 °C, **PP-PAF** was obtained as grey solid in 85% yield.

Synthesis of PP_C-PPy_S-PAF-1: A mixture of 1,3,5-Tris(4-bromophenyl)benzene (TBrPB) (100 mg, 0.185 mmol), and benzene-1,4-diboronic acid (BDDBA) (92 mg, 0.555 mmol) in DMF (15 mL) was degassed by three freeze–pump–thaw cycles. To the mixture was added an aqueous solution of K₂CO₃ (2.0 M, 1.0 mL) and Pd(PPh₃)₄ (15.0 mg). The mixture was degassed by three freeze–pump–thaw cycles, and purged with N₂, and stirred at 90 °C for 12 h. The mixture was allowed to cool at room temperature, and was added with a mixture of 1,3,6,8-tetrabromopyrene (0.023 mmol, 12mg) and catalyst (2 M K₂CO₃, 0.4mL and Pd(PPh₃)₄ 9 mg). The resulting mixture was degassed by three freeze–pump–thaw cycles purged with N₂, and stirred at 120 °C for 2 days. The precipitate was filtered, washed with water, methanol, THF, and DMF. Further purification was carried out by Soxhlet extraction with methanol and THF for 48 h, respectively. After dried in a vacuum oven at 150 °C, **PP_C-PPy_S-PAF-1** was obtained as grey solid in 87% yield.

For the synthesis of **PP_C-PPy_S-PAF-2** and **PP_C-PPy_S-PAF-3**, the same reaction procedure was performed unless the added with 1,3,6,8-tetrabromopyrene was 0.046 mmol and 0.092 mmol, respectively.

Fluorescence study: Before testing, 10 mg of PAFs is weighed and added to a bottle containing 10 mL of ethanol under stirring to form homo-disperse solution. In typical experimental setup, 0.5 mL above-mentioned solution was added to cuvette containing 1.5 mL of ethanol. The fluorescence upon excitation at required wavelength was measured in-situ after incremental addition of freshly prepared analyte solutions. All the experiments were performed in triplicate and consistent results are reported.

Preparation of test strips.

For making the test strips of the sample, the double-sided tapes were paste on dry quartz (or glass) slides. The powder of PAFs was then evenly sprinkled onto the surfaces of the tapes. After covered by another slide, the “sandwich” was pressed and rotated to make the sample intrude into the glue of tape. Then the tape was ultrasound in ethanol to remove any powder that was not glued well on the tape. After rinsing with ethanol and drying in the air, the test strips was made.

Preparation of vapor phase detecting thin layers.

A thin layer of PP_C-PPy_S-PAF-2 was prepared using the method reported by Li etc.^[S2] Quartz slides were rinsed by de-ionized water and ethanol and dried by nitrogen flow. Double-sided tapes were then applied to the slides. The tapes were peeled off after a few minutes. The activated powder of PAFs was then evenly sprinkled onto the surfaces of the slides. The slides were blow by nitrogen flow to remove any powder that was not glued well to the surface of the slides. Then the slides were applied to the vapor phase detecting.

For vapor phase detection, the thin layer was exposed to analyte vapor in a closed jar. Fluorescent spectra of samples before and after exposure to various analyte vapors were collected at 5 minutes.

[S2]. A. Lan, K. Li, H. Wu, D. H. Olson, T. J. Emge, W. Ki, M. Hong, and J. Li, *Angew. Chem. Int. Ed.* 2009, 48, 2334-2338.

4.Theoretical methods.

The molecular orbital levels are generated after structural optimization and vibrational analysis. The calculations were performed at the density functional (DFT) level of theory using the 6-311++G* basis set [1,2] and the hybrid B3LYP functional, [3] was employed. The vibrational analysis were used to confirm the nature of the stationary points. All calculations were carried out with the Gaussian 09 suite of programs.[4]

[S3] A. D. McLean and G. S. Chandler, "Contracted Gaussian-basis sets for molecular calculations. 1. 2nd row atoms, Z=11-18," *J. Chem. Phys.*, 1980, 72, 5639-5648.

[S4] K. Raghavachari, J. S. Binkley, R. Seeger, J. A. Pople, "Self-Consistent Molecular Orbital Methods. 20. Basis set for correlated wave-functions," *J. Chem. Phys.*, 1980, 72, 650-654.

[S5] A.D. Becke, *J.Chem.Phys.* 1993, 98, 5648-5652; C. Lee, W. Yang, R.G. Parr, *Phys. Rev. B*, 1988, 37 785-789; S.H. Vosko, L. Wilk, M. Nusair, *Can. J. Phys.*, 1980, 58, 1200-1211; P.J. Stephens, F.J. Devlin, C.F. Chabalowski, M.J. Frisch, *J.Phys.Chem.* 1994, 98, 11623-11627.

[S6] Gaussian 09, Revision C.01, M. J. Frisch, G. W. Trucks, H. B. Schlegel, G. E. Scuseria, M. A. Robb, J. R. Cheeseman, G. Scalmani, V. Barone, B. Mennucci, G. A. Petersson, H. Nakatsuji, M. Caricato, X. Li, H. P. Hratchian, A. F. Izmaylov, J. Bloino, G. Zheng, J. L. Sonnenberg, M. Hada, M. Ehara, K. Toyota, R. Fukuda, J. Hasegawa, M. Ishida, T. Nakajima, Y. Honda, O. Kitao, H. Nakai, T. Vreven, J. A. Montgomery, Jr., J. E. Peralta, F. Ogliaro, M. Bearpark, J. J. Heyd, E. Brothers, K. N. Kudin, V. N. Staroverov, R. Kobayashi, J. Normand, K. Raghavachari, A. Rendell, J. C. Burant, S. S. Iyengar, J. Tomasi, M. Cossi, N. Rega, J. M. Millam, M. Klene, J. E. Knox, J. B. Cross, V. Bakken, C. Adamo, J. Jaramillo, R. Gomperts,

R. E. Stratmann, O. Yazyev, A. J. Austin, R. Cammi, C. Pomelli, J. W. Ochterski, R. L. Martin, K. Morokuma, V. G. Zakrzewski, G. A. Voth, P. Salvador, J. J. Dannenberg, S. Dapprich, A. D. Daniels, Ö. Farkas, J. B. Foresman, J. V. Ortiz, J. Cioslowski, and D. J. Fox, Gaussian, Inc., Wallingford CT, 2009.

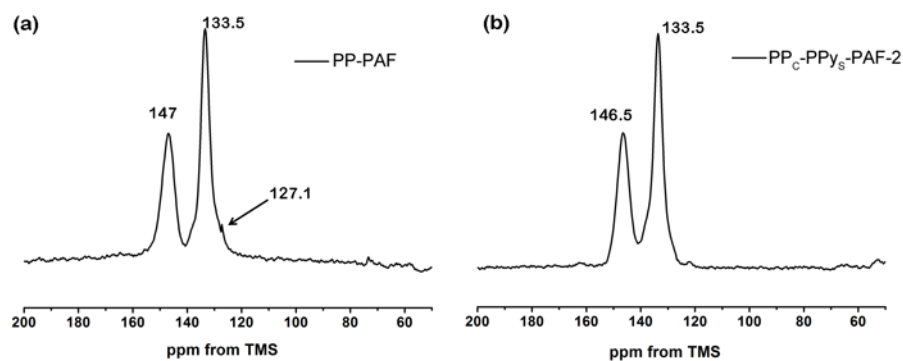


Figure S1: Solid-state ^{13}C NMR of PP-PAF (a) and PP_c-PPy_S-PAF-2 (b).

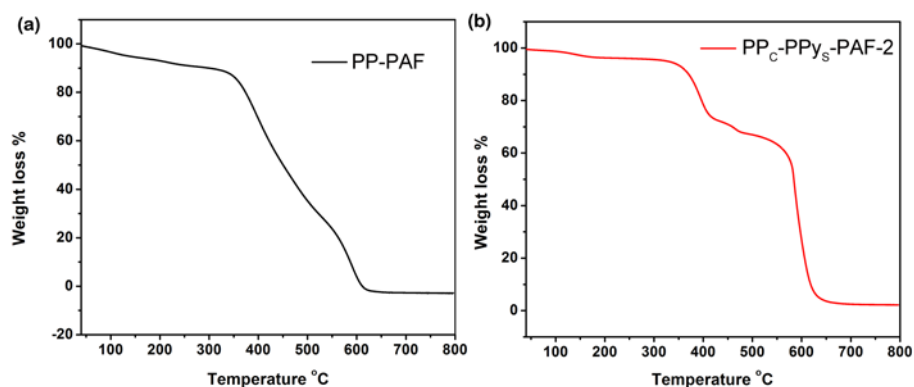


Figure S2: TGA plots of PP-PAF and PP_c-PPy_S-PAF-2 under air conditions.

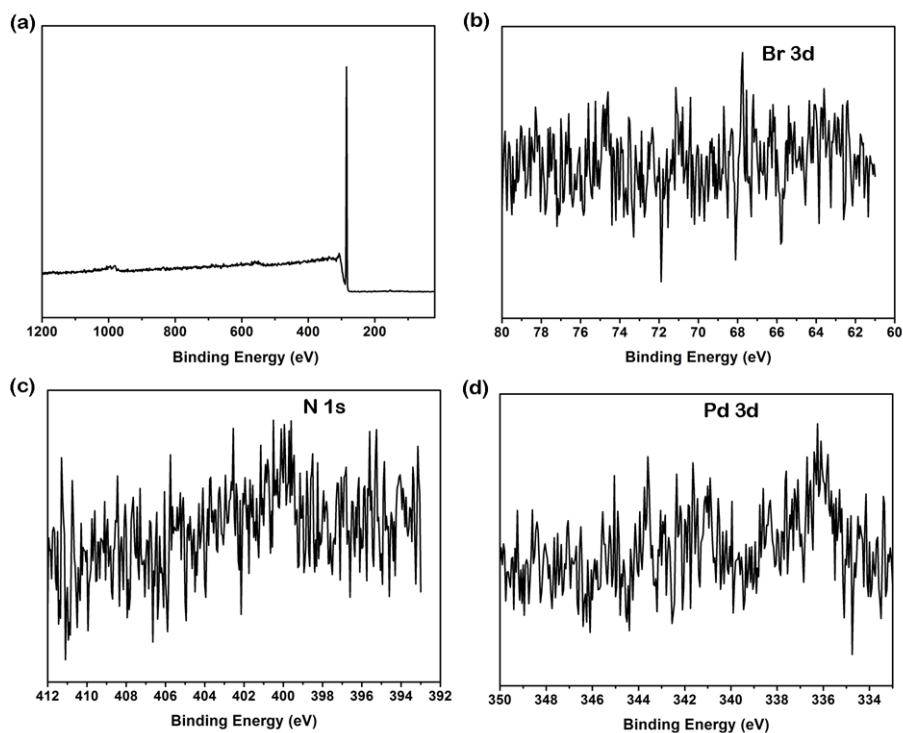


Figure S3: XPS spectrum of PP_c-PPy_s-PAF-2.

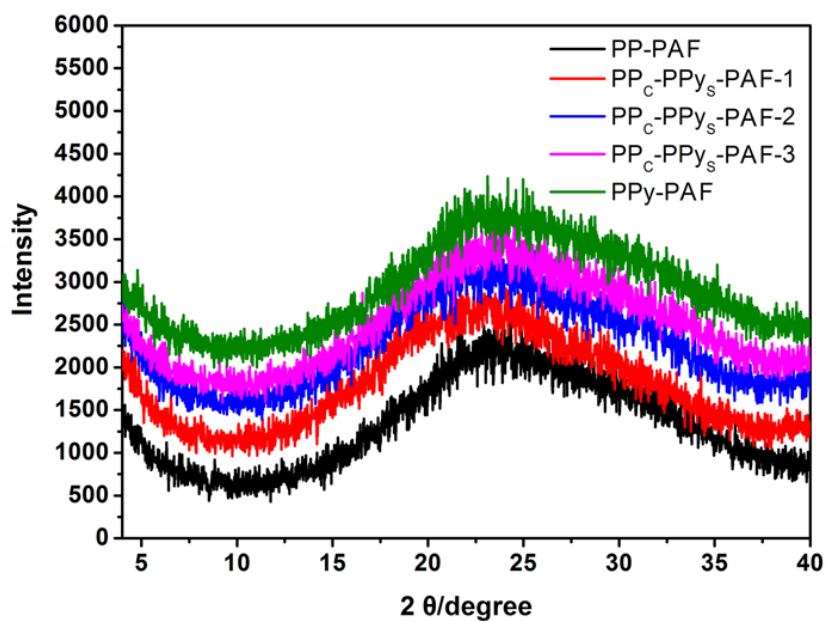


Figure S4: Powder X-ray diffraction patterns of PP-PAF and PP_c-PPy_s-PAFs.

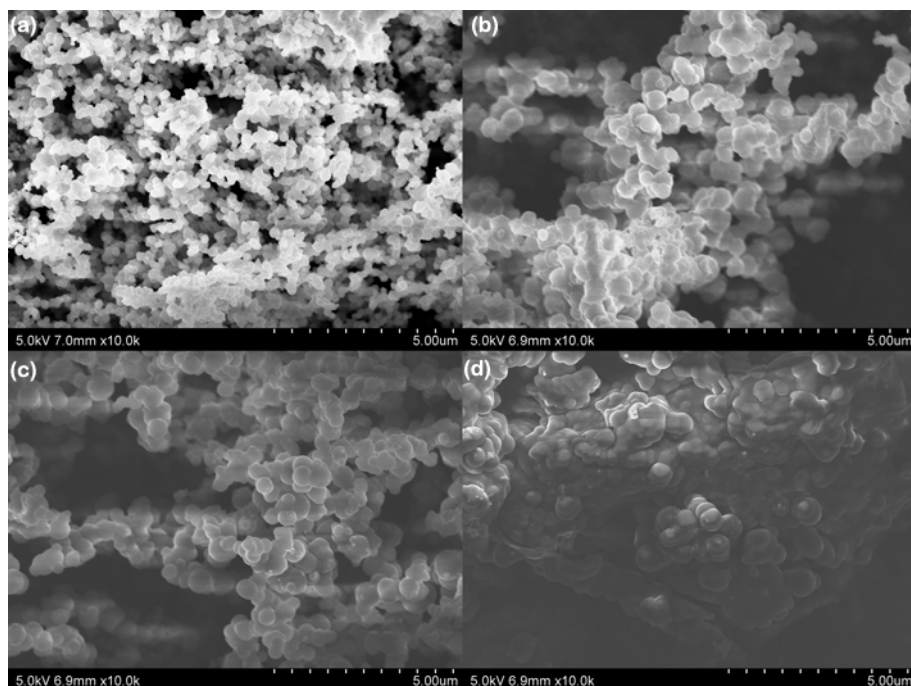


Figure S5: SEM images of PP-PAF (a), PP_C-PPy_S-PAF-1(b), PP_C-PPy_S-PAF-2 (c) and PP_C-PPy_S-PAF-3 (d).

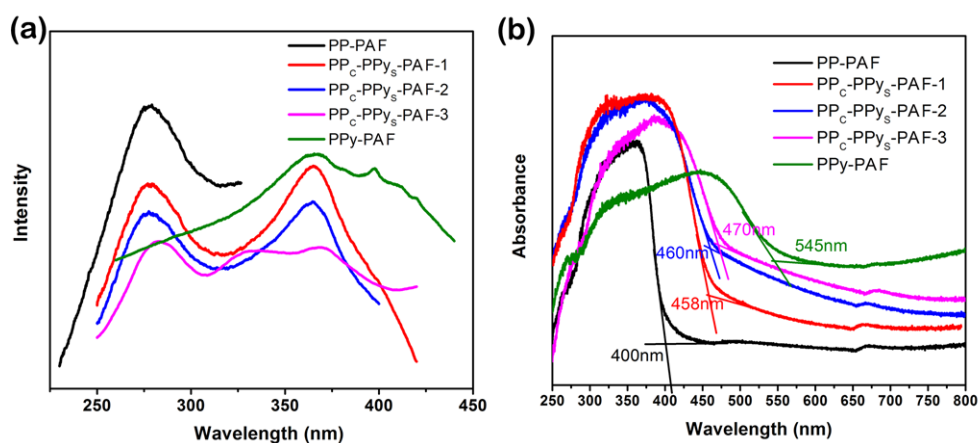


Figure S6: a) Excitation spectra of PP-PAF, PPy-PAF and PP_C-PPy_S-PAFs, at the maximum emission, respectively; b) Absorption band of PP-PAF, PPy-PAF and PP_C-PPy_S-PAFs.

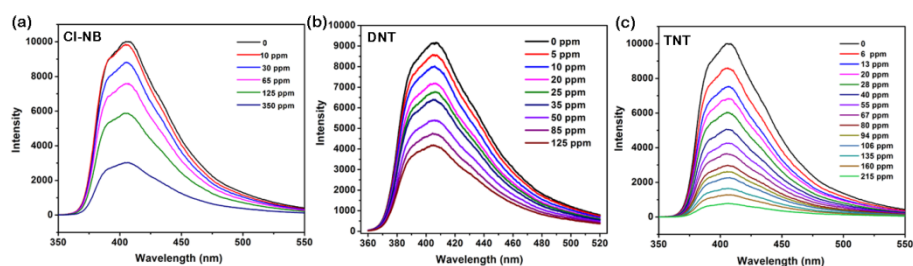


Figure S7: Emission spectra of PP-PAF upon incremental addition of CI-NB, DNT and TNT solution in ethanol.

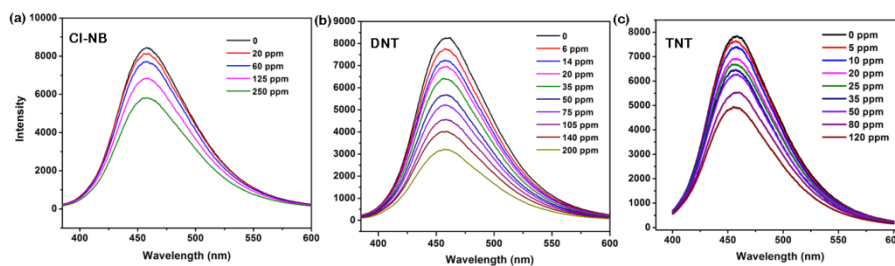


Figure S8: Emission spectra of PP_C-PPy_S-PAF-1 upon incremental addition of Cl-NB, DNT and TNT solution in ethanol.

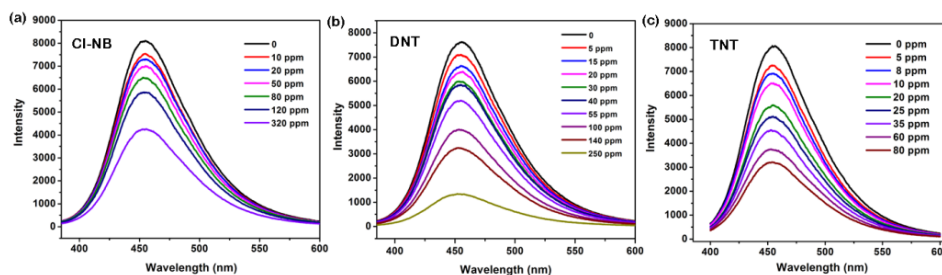


Figure S9: Emission spectra of PP_C-PPy_S-PAF-2 upon incremental addition of Cl-NB, DNT and TNT solution in ethanol.

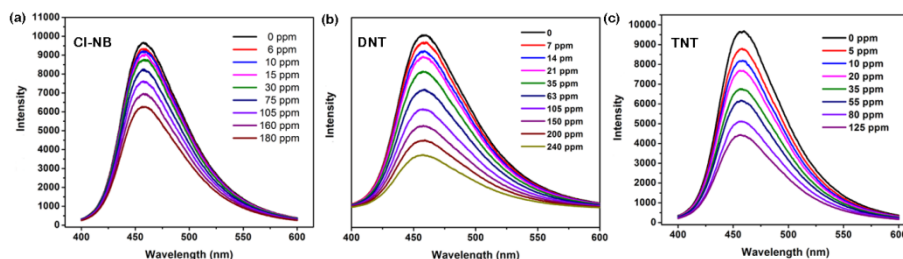


Figure S10: Emission spectra of PP_C-PPy_S-PAF-3 upon incremental addition of Cl-NB, DNT and TNT solution in ethanol.

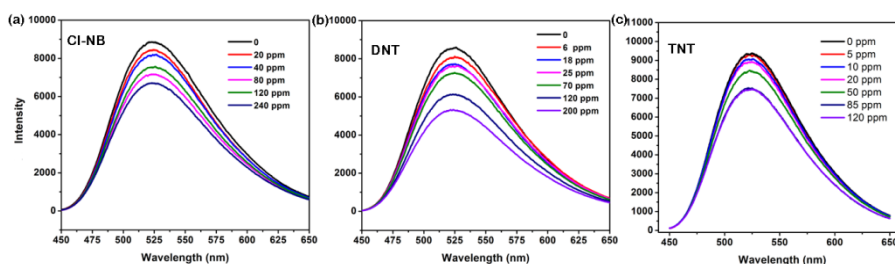


Figure S11: Emission spectra of PPy-PAF upon incremental addition of Cl-NB, DNT and TNT solution in ethanol.

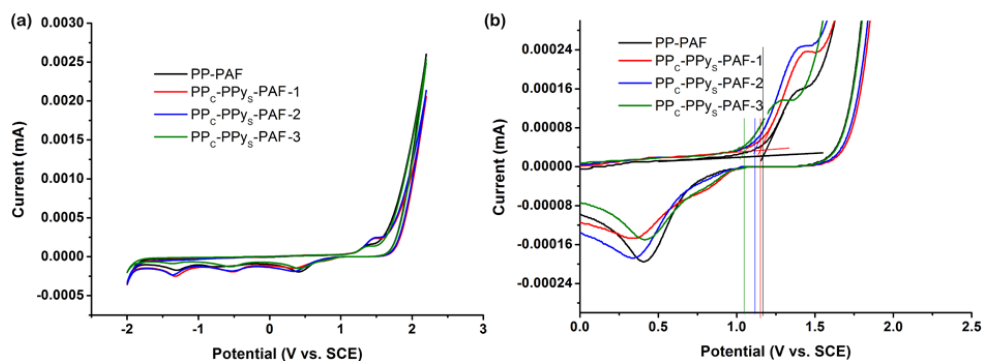


Figure S12: Cyclic voltammograms of PP-PAF and PP_c-PPy_S-PAFs. (a) The cyclic voltammograms obtained at 50 mV/s in methylene chloride solution and 0.1M Tetrabutylammonium Perchlorate. Working electrode was glassy carbon auxiliary electrode platinum electrode, a reference electrode is a saturated calomel electrode; (b) Zoom of the voltammogram as shown in (a).

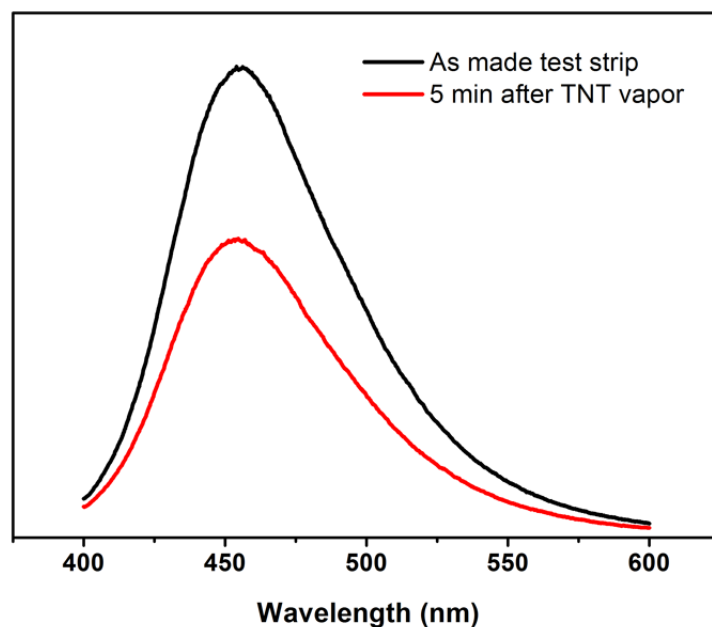


Figure S13: Emission spectra of PP_c-PPy_S-PAF-2 paper test strip before and after exposure to TNT vapor for 5 minutes.

Table S1. The PL and electrochemical properties of the PP-PAF, PPy-PAF and PP_C-PPy_S-PAFs

PAFs	PL peaks [nm]	PL QY	$E_{ox}[V]^a$	HOMO [eV] ^b	LUMO [eV] ^b	$E_g[eV]^c$
PP-PAF	409	0.1	1.17	-5.91	-2.8	3.1
PP _C -PPy _S -PAF-1	452	0.1	1.15	-5.89	-3.18	2.71
PP _C -PPy _S -PAF-2	455	0.13	1.13	-5.87	-3.19	2.68
PP _C -PPy _S -PAF-3	459	0.17	1.09	-5.83	-3.21	2.62
PPy-PAF	525	0.05	-	-	-	2.27

^a) Oxidation potentials measured by cyclic voltammetry; ^b) HOMO= $-e(E_{ox}+4.74\text{ V})$; ^c) LUMO = HOMO- E_g ; ^d) E_g estimated from the UV-Vis absorption spectra.

Table S2: HOMO and LUMO energies calculated for explosive analytes (at B3LYP/6-31G* level of theory).

Analytes	HOMO (eV)	LUMO (eV)	$E_g[eV]^c$
NT	-7.68	-2.789	4.891
Cl-NB	-7.862	-3.105	4.757
DNT	-7.764	-3.23	4.534
TNT	-8.83	-3.868	4.962
TNP	-8.595	-4.321	4.274